frontiers | Frontiers in Biophysics

TYPE Original Research
PUBLISHED 25 April 2025
DOI 10.3389/frbis.2025.1543172

OPEN ACCESS

EDITED BY
Gustavo Chaves,
Paracelsus Medical Private University, Germany

REVIEWED BY
Bernardo Pinto,
The University of Chicago, United States
Derek P. Claxton,
Vanderbilt University, United States

*CORRESPONDENCE
J. F. Ek-Vitorin,
ekvitori@arizona.edu

RECEIVED 11 December 2024
ACCEPTED 31 March 2025
PUBLISHED 25 April 2025

CITATION
Ek-Vitorin JF, Shahidullah M and Delamere NA (2025) Activation of transient receptor vanilloid 4 increases connexin hemichannel activity in porcine ciliary nonpigmented epithelium. *Front. Biophys.* 3:1543172.
doi: 10.3389/frbis.2025.1543172

Activation of transient receptor vanilloid 4 increases connexin hemichannel activity in porcine ciliary nonpigmented epithelium

J. F. Ek-Vitorin[1]*, M. Shahidullah[1,2] and N. A. Delamere[1,2]

[1]Department of Physiology, University of Arizona, Tucson, AZ, United States, [2]Department of Ophthalmology and Vision Science, University of Arizona, Tucson, AZ, United States

The ciliary nonpigmented epithelium (NPE) is responsible for the secretion of the aqueous humor into the eye. Indirect evidence from earlier studies raised the possibility that unpaired NPE connexins might form functional hemichannels. Here we used a patch clamp approach to confirm the presence of functional NPE hemichannels on the basis of electrical conductance. We also examined responses to TRPV4 activation because it has been suggested that TRPV4 activation can cause connexin hemichannels to open. Studies using whole-cell (WC) patch clamp showed that hemichannel-like conductance transitions appear spontaneously at a positive holding potential (+80 mV). Most of the transitions fell in the 180–240 pS range expected for fully open Cx43 hemichannels. Activation of TRPV4 channels with the agonist GSK1016790A (10 nM) increased the open probability of the presumptive hemichannels and shifted their conductance toward lower amplitudes. Cell-attached (CA) patch clamp recordings also showed events with low conductance values that signify partially open hemichannels. GSK1016790A exposure also induced depolarization, a response causally associated with hemichannel opening. In studies on coupled pairs of cells, gap junction channel full open conductance amplitudes corresponded to values reported for Cx43, and approximately half the conductance of the observed hemichannel-like events, consistent with the notion that Cx43 is responsible for the observed hemichannels. Taken together, the findings are consistent with NPE hemichannels, formed by Cx43, that open in response to TRPV4 activation. While it seems likely that Ca^{2+} entry plays a role in the hemichannel response to TRPV4 activation, the depolarization that occurs upon TRPV4 activation might also be important.

KEYWORDS

ciliary epithelium, hemichannels, TRPV4, patch clamp, connexin, aqueous humor

1 Introduction

Aqueous humor is formed by the ciliary body, a specialized musculoepithelial structure located in an area between the posterior of the iris root and the margin of the retina. The elaborately folded surface of the ciliary body is covered by an epithelial cell bilayer. One type of epithelial cell, ciliary nonpigmented epithelium (NPE) faces the aqueous humor in the interior of the eye. A different type of epithelial cell, ciliary pigmented epithelium (PE) faces the network of leaky blood vessels inside the ciliary body. Transport mechanisms in the

two cell layers operate in a coordinated manner to produce aqueous humor by transporting ions and water from the blood-side into the posterior chamber of the eye. This is made possible because the NPE and PE are coupled by gap junctions located where the apical surfaces of each cell makes contact. Accordingly, there is abundant expression of connexin protein at the apical surfaces of the NPE and PE. However, there is also rich connexin expression at the basolateral surface of the NPE where the cells contact extracellular fluid, the aqueous humor. Obviously, these connexins are unpaired. Earlier studies were conducted using propidium iodide (MW 668) to determine whether the unpaired NPE connexins might form functional hemichannels. Evidence for hemichannel opening was as follows: propidium iodide added to the aqueous humor was observed to enter the NPE under low external calcium conditions and the movement was prevented by the nonselective connexin inhibitor 18α-glycyrrhetinic acid (Shahidullah and Delamere, 2014). The present study was to confirm functional hemichannel events by a more direct approach using patch clamp.

NPE connexins have been characterized to some extent. Native and cultured porcine NPE cells express both Cx43 and Cx50 (Shahidullah and Delamere, 2014). The NPE also expresses the transient receptor potential vanilloid 4 (TRPV4) channels at the basolateral surface (Shahidullah and Delamere, 2023). This is intriguing because recently published studies demonstrate that activation of TRPV4 can cause connexin hemichannels opening (Ek-Vitorin et al., 2023). The role of TRPV4 and connexin hemichannels in NPE cells remains to be determined but we speculate that they might be involved in coordinating transporter activity in the two ciliary epithelium cell types. In the lens, TRPV4 activation and hemichannel opening in response to osmotic swelling are critical steps in a feedback mechanism that regulates Na,K-ATPase activity (Shahidullah et al., 2012a; Shahidullah et al., 2012b). In the ciliary epithelium bilayer Na,K-ATPase is located mainly at the NPE basolateral surface where the expression of multiple different isoforms of the Na,K-ATPase catalytic subunit points to a highly specialized active Na-K transport mechanism (Ghosh et al., 1991; Riley and Kishida, 1986). Na,K-ATPase activity establishes ion gradients that drive different secondary active transport mechanisms at the basolateral surfaces of the NPE and PE cells. Aqueous humor secretion occurs because the coordinated action of these transporters and associated ion channels drives the movement of solutes and osmotically associated water in a blood to aqueous direction. At steady-state, the rate of solute and water entering the PE layer must be matched by an equal rate of exit from the NPE. A mismatch would lead to swelling or shrinkage of the cells in the bilayer. Earlier, we suggested that the mechanosensitive TRPV4 channel at the NPE basolateral surface might respond to cell swelling and initiate a response that activates hemichannels and perhaps regulates Na,K-ATPase activity (Shahidullah and Delamere, 2023). That is to say, TRPV4 activation and an increased hemichannel opening could have functional consequences in the regulation of aqueous humor production.

Cx43 was shown abundantly at the junction between the NPE and PE layers, where gap junctions couple both cell types, while Cx50 was evident at the aqueous humor-facing, basolateral side of NPE (Shahidullah and Delamere, 2014). Mechanical stimulation of NPE cells caused ATP release that was prevented by the nonselective connexin blocker glycyrrhetinic acid, by a connexin mimetic peptide GAP27, and by a TRPV4 antagonist (Shahidullah and Delamere, 2023; Shahidullah et al., 2012a). Here, using electrophysiological techniques, and based on their expected electrical conductance, we provide proof of the presence of connexin hemichannels in NPE cells. We also examined their responses to TRPV4 activation because earlier studies, including some in the lens (Ek-Vitorin et al., 2023), suggested TRPV4 activation can cause connexin hemichannels to open. One additional goal of these studies is to determine whether the functional interaction between TRPV4 and Cx43, as observed in lens, exists in other cell types.

2 Methods

2.1 Cells

Nonpigmented ciliary epithelial cells were isolated from porcine eyes and established in primary culture using a method described previously (Shahidullah et al., 2007). Characterization of cell phenotype based on expression of markers such as Na,K-ATPase isoforms and nitric oxide synthases was also described earlier (Shahidullah et al., 2007). Cells were used up to passage five. For electrophysiological studies, cells were separated by trypsinization and plated on glass coverslips, either at low density by dilution, or at high density by depositing a single small drop of medium in the center of the dry coverslip and allowing cells to settle for 1–2 h in the incubator before adding more medium. Using this "drop" method, we obtained groups of cells. Single cells could be found around the central dense groups in the "drop" method, or in low density plating.

2.2 Electrophysiology

Coverslips with attached NPE cells were positioned in a recording chamber on the stage of an upright microscope (BX50WI, Olympus). Recordings were made using a pair of discontinuous single-electrode voltage-clamp (DSEVC) amplifiers (SEC-05LX NPI, Germany) (Ek-Vitorin and Burt, 2005). For measurements of total membrane current (I_m) and resting membrane potential (RMP), K^+-containing solutions were used, both externally (in mM: NaCl 140, KCl 4.7, CaCl2 1.8, $MgCl_2$ 1.2, EGTA 0.1, Glucose 10, HEPES 10; adjusted to pH = 7.2, and 319–330 mOsm) and internally (in mM: KCl 124, $MgCl_2$ 3, TEACl 9, $CaCl_2$ 0.5, EGTA 9, Glucose 5, Na2 ATP 5, HEPES 9; adjusted to pH = 7.4, and 315–319 mOsm). To decrease membrane currents and promote the visualization of hemichannel-like events, K^+ currents were prevented by partially substituting Cs^+; additionally, NaCl and KCl concentrations were adjusted to preserve osmolarity, while keeping all the other components intact. Thus, the external solution composition became (in mM) NaCl 125, 4 KCl, 15 CsCl, and that of the internal solution (in mM) 125 KCl, 14 CsCl. Patch clamp recordings were made as described below and test drugs were introduced after first establishing a control baseline. Specifically, the TRPV4 agonist GSK1016790A (GSK) was applied by slow drip of 1 mL of solution into 4 mL of bathing solution already in the recording chamber to a final concentration of 10 nM. Current and voltage values were compared before (control) and after drug application.

Patch pipettes with resistance values of 3–10 MΩ when filled with the selected solutions, were lowered onto an isolated cell, or a cell within a group, and a high resistance (Gigaohm, GΩ) seal was obtained between the electrode tip and a patch of membrane. The membrane patch was then either broken with negative pressure to achieve the whole-cell (WC) configuration and record total I_m, or left intact in a cell-attached (CA) configuration to record channel activity exclusively in that fragment of cell membrane. The WC/CA configuration combines both modes with two electrodes in a single isolated cell. For the recording of gap junction channels, two paired cells were held each in WC configuration, and transjunctional voltage (V_j) gradients were imposed between the cells, as previously described (Ek-Vitorin and Burt, 2005). Manual measurements of channel amplitude were performed as customary (Ek-Vitorin and Burt, 2005; Ek-Vitorin et al., 2006), using the cursor properties in Clampfit (pCLAMP 10); briefly, for every current transition denoting an open channel, a cursor was placed at the base and another at the top of the channel opening, or *vice versa* for closing transitions, and the current differential (ΔI_m) thus recorded was used to calculate the change in channel conductance ($\Delta I_m/V_m = \gamma$; $\Delta I_j/V_j = \gamma_j$), that is, the transition conductance. For some short I_m trace fragments, all-points histograms (showing the relative frequency of every current level) are provided for comparison purposes.

Pulsing protocols were variable length pulses to zero, −80 and +80 mV, and sustained clamping at holding potential (V_{hold}) of −50 mV (Ek-Vitorin et al., 2023). Cs^+-containing solutions were used to decrease K^+-like currents, particularly at +80 mV. Under these conditions, negative voltages generate small inward currents, while positive voltages induce comparatively larger currents that often display channel-like events. Initially, the whole cell membrane currents (WC I_m) in response to short pulses of −80 and +80 mV were recorded, and the quality of the seals certified by the small "leak" currents and the narrow capacitive artifact at either voltage polarity (Supplementary Figure S1). Only experiments with proper seal quality were continued and considered for analysis. Gap junction channel amplitudes were measured as before (Ek-Vitorin and Burt, 2005) with applied transjunctional voltages (V_j) of ±40 and ±80 mV. In addition, *I-V* curves were obtained with 20 mV stepwise square pulse protocols, from highly negative (−90 or −80 mV) to highly positive (+80 or +90 mV) voltages. In macroscopic recordings, for each trace, instantaneous currents (Inst I_m) were measured during the first 30 ms of recording after the beginning of the pulses, and steady-state currents (SS I_m) were the average of the last 200 ms. Resting membrane potential (RMP) was measured in Bridge Mode (no voltage clamping). Values are reported as Mean ± SEM. Open probability (P_o) and the number of open channels (NP_o) were calculated automatically using Clampfit analysis of suitable segments of recording before and after GSK application.

3 Results

3.1 Spontaneous hemichannel-like activity

Whole-cell patch clamp recordings are the gold standard approach to detect connexin hemichannels, especially when recordings are made in the absence of other currents. Commonly, connexin channels are relatively large, they gate slower than typical ion channels, and display substates (Supplementary Figure S2) that may relate to their permeability to large molecules (Ek-Vitorin and Burt, 2005; Ek-Vitorin et al., 2006). NPE cells express both Cx43 and Cx50 (Shahidullah and Delamere, 2014). The conductance of gap junction channels composed by these connexins (Ek-Vitorin and Burt, 2013; Harris, 2001), and therefore the expected conductance of their unpaired connexons (or hemichannels) are well known. To emphasize, for any connexin, the conductance of their unpaired hemichannel is roughly twice the conductance of a gap junction channel. Cx43 hemichannels are expected to have a maximal conductance of ~240 pS (Harris, 2001; Ek Vitorín et al., 2016), and those of Cx50, ~400 pS (Harris, 2001; Srinivas et al., 1999). Previous data (Ek-Vitorin et al., 2023) suggested we would detect Cx43 hemichannels at high positive voltages (Contreras et al., 2003a). Cx50 hemichannels may not open at positive (Ebihara et al., 1999; Hopperstad et al., 2000) but at negative membrane voltages (Beahm and Hall, 2002) (see Discussion). We thus asked whether NPE cell membranes display hemichannel-like events in control conditions, and this was the case.

In the first series of experiments, K^+ channel activity was suppressed by including Cs^+ in both the bathing solution and the solution in the patch pipette. When single NPE cells were switched between holding potentials of zero, −80 and +80 mV hemichannel-like activity was evident as currents that signified opening of large conductance channels at +80 mV (Figure 1), but no channels of similar amplitudes were seen at −80 mV. The hemichannel activity observed in different cells showed variability. For example, in the simultaneous recordings shown in Figure 1, chosen to fully illustrate the range of the aforementioned variability, the presence of channel-like transitions compatible with fully open Cx43 hemichannels (228 and 253 pS) was immediately obvious in 1 cell (labeled WC-2), but not in the other (labeled WC-1), which showed smaller events <100 pS (Figures 1C, D). When +80 mV pulses of longer duration were applied to both cells (Figure 2), WC-1 displayed a few hemichannel-like transitions (~246 pS) several minutes into the recording (Figure 2A, pulse 3), while in WC-2 the channel activity continually increased (Figure 2B). In general, the longer the voltage pulse the larger the current buildup, until transitions became unrecognizable (Figures 2B–D). Interestingly, after increasing at +80 mV, the whole cell I_m regularly returned to initial levels on pulsing to −80 mV.

We then asked whether, under conditions of K^+ channel blockade by Cs^+, the hemichannels present could open sufficiently fast to generate a measurable membrane current when applying short pulses of increasing strength. This would agree with data showing increasing membrane currents at large positive voltages mediated by Cx43 hemichannels (Contreras et al., 2003a). When a stepwise protocol of 5-second pulses of increasing voltage was applied, the cell with the largest presence of hemichannel-like events also showed an increase of steady-state I_m at voltages >50 mV (Figure 3). Because of the presence of Cs^+ in the solutions, these currents are unlikely to be carried by K^+ ions.

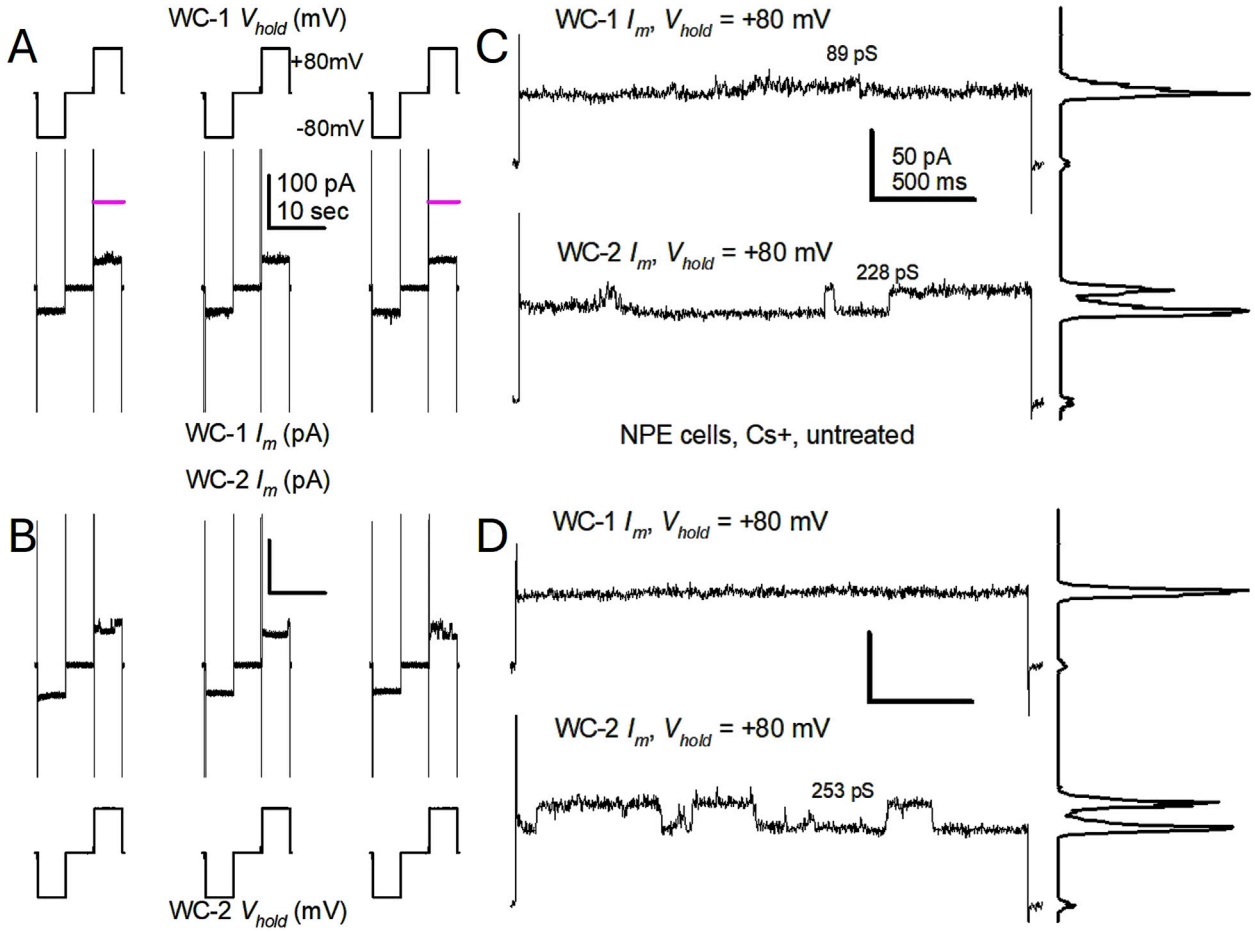

FIGURE 1
Untreated, single porcine Non-Pigmented Epithelial (NPE) cells display spontaneous channel events resembling Cx43 hemichannels at +80 mV. **(A, B)** Simultaneous patch clamp recordings of the whole cell membrane current from two single NPE cells subjected to repeated, 5 s long, ±80 pulses in cesium (Cs^+)-containing solutions. Only three pulses are shown. In **(A)**, V_m pulses are at the top and the resultant whole cell currents (WC I_m) at the bottom; in **(B)**, the order is reversed for ease of I_m comparison. Notice the small leak currents and large capacitive currents (cropped), denoting tight seals and large cells, respectively. Channel-like events, the appearances of which are magnified in the next panels, are readily seen in cell 2 (WC-2 I_m), but not in cell1 (WC-1 I_m). I_m calibration in **(A)** applies to **(B)**. **(C, D)** Close-ups of WC I_m at +80 mV from cells in **(A)** and **(B)**. For both cells, traces are taken from the time indicated (pink lines) in **(A)**; **(C)** is from the first displayed pulses, **(D)** is from the third displayed pulses. Channels of amplitude compatible with Cx43 hemichannels were seen in cell 2, but not in cell 1. The plots to the right of each trace are all-points histograms, and the calculated channel conductance (γ) in picosiemens (pS) for the transitions between current levels is shown near the traces. The presence of Cs^+ in both internal and external solutions prevents the function of K^+ channels. I_m calibration in **(C)** applies to **(D)**.

However, single event transitions are not easily identified in these traces.

At this stage, we demonstrated that NPE cell membranes display hemichannel-like events in control conditions. While we cannot explain the variability of hemichannel activity, it might reflect disparate levels of connexin expression or hemichannel activation in individual cells. Due to this inconsistent channel activity, an average of the currents recorded from more than 20 cells in control conditions would be deceptive. More significantly, every NPE cell recorded in control conditions displayed some level of hemichannel-like activity, with transitions like those illustrated in Figures 1, 2 (and Supplementary Figures S1, S2). We next asked whether TRPV4 activation increased this hemichannel-like activity.

3.2 TRPV4 activation increased hemichannel open probability and decreased transition amplitude

The selective TRPV4 agonist GSK1016790A (GSK) was applied by slow drip of 1 mL of solution onto 4 mL already in the recording chamber, to a final GSK concentration of 10 nM. Shortly after the application of GSK, NPE cells held at +80 mV displayed I_m increases of more than 10-fold, from 138.2 ± 72.3 to 1537.8 ± 622.5 pA (n = 9). Interestingly, cells held at negative voltage did not show such a large I_m increase, possibly because Cx43 hemichannels remain closed at negative voltages (see Discussion). This observation also argues against the opening of Cx50 hemichannels, which might be expected to remain open at negative voltages (Ebihara et al., 1999; Hopperstad et al., 2000; Beahm and Hall, 2002).

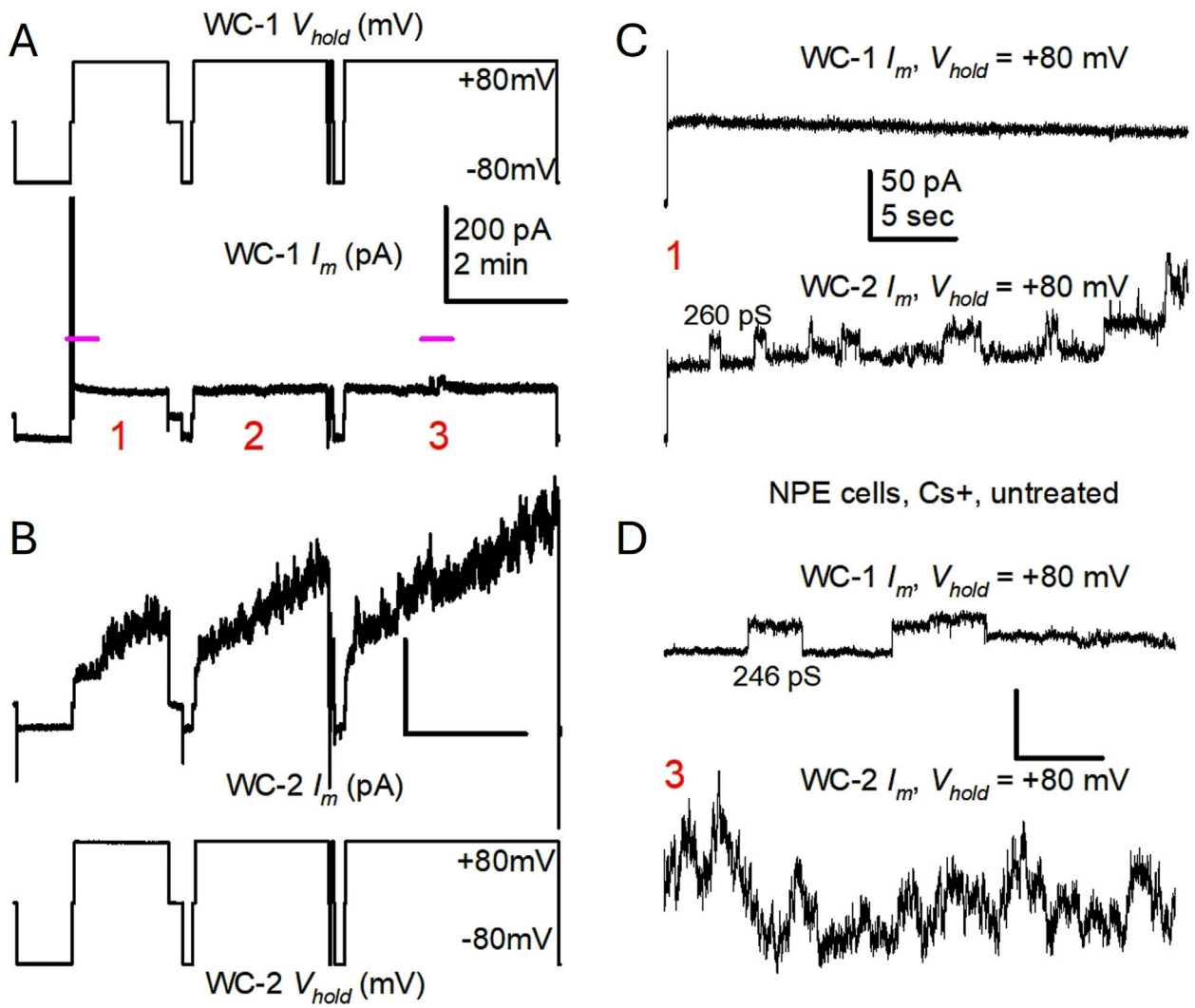

FIGURE 2
Untreated, single porcine NPE cells display variable frequency of Cx43 hemichannel-like events during long +80 mV pulses. **(A, B)** Simultaneous patch clamp recordings from two single cells (same as in Figure 1), during long membrane polarizations at +80 mV (traces tagged as in Figure 1), showing three separate pulsing episodes (labeled 1–3). Notice that cell 1 I_m displayed only a few channel events in the middle of pulse episode three (pink line), while cell 2 I_m continuously increased during each of the three pulses illustrated. I_m calibration in **(A)** applies to **(B)**. **(C, D)** Close-ups of short stretches (marked in A with pink lines) during the first and third +80 mV pulse episodes, respectively, further illustrating the difference in channel opening frequency between the 2 cells. The calculated γ values for some I_m transitions are provided. Notice that some openings are not followed by complete closures to the previous baseline [bottom trace in **(C)**, top trace in **(D)**], but to an intermediate or residual state that seems to remain for a long time. Also notice that as I_m becomes larger, single events are less recognizable. I_m calibration in **(C)** applies to **(D)**.

The large I_m triggered by GSK at +80 mV was not conducive to the recognition of channel events, the main indicator in our study. To be explicit, calculation of open probability and measurements of channel amplitude can only be performed when channels are clearly defined, in our case, before I_m becomes unmanageable. However, in some cases the response to GSK was relatively modest, and some delay after GSK exposure preceded persistent increases of I_m. Interestingly, the nature of the presumptive hemichannel events seemed to change during that brief time: transitions appear more abundant but smaller (Figure 4). In the case illustrated in Figure 4, NP_o for five identifiable current levels was 0.89 in the absence of GSK, while NP_o for six identifiable currents levels was 2.47 in the presence of GSK (Figures 4A–C). More significantly, the amplitude of current transitions appear to decrease. Manual measurements during the time before the large I_m increase demonstrated channel transitions in the conductance range 80–300 pS (Figures 4D–F). Some large transitions fell outside the 180–240 pS range expected for fully open Cx43 hemichannels (Contreras et al., 2003a; Contreras et al., 2003b). Furthermore, the small conductance transitions became more frequent after GSK treatment (Figures 4C–F). The combined occurrence of multiple apparent openings, more frequent small transitions, and overall increase of I_m, contributed to a "noisier" appearance of the recording in cells exposed to GSK (Figure 4C). We cannot state with certainty that the subsequent I_m increases (Figure 4A) are due to largescale hemichannel opening, but if this was the case, GSK might be altering hemichannel open probability and conductance.

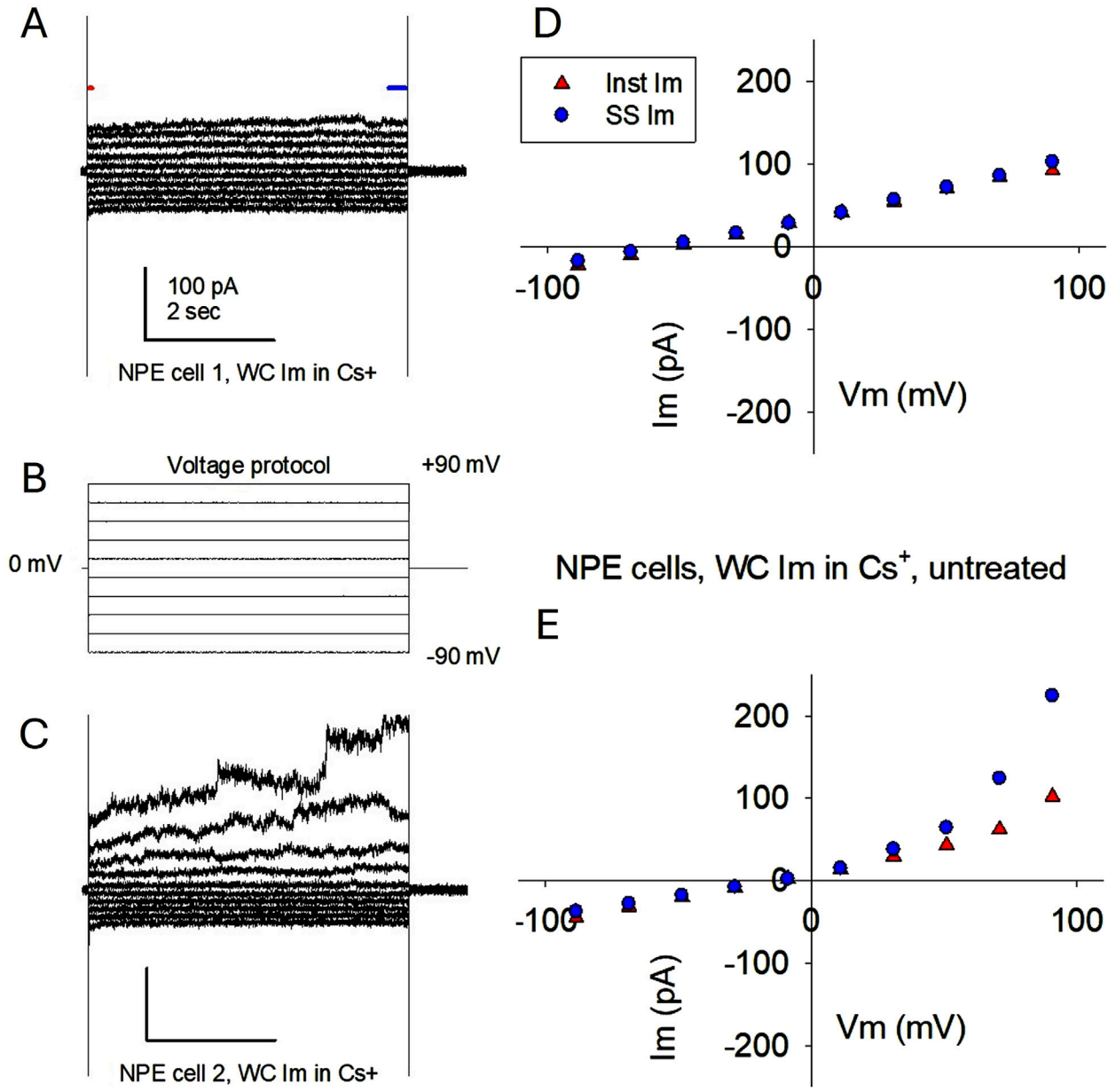

FIGURE 3
Membrane currents elicited in single porcine NPE cells by a stepwise voltage protocol are compatible with hemichannel currents. **(A–C)** Applied voltage protocol **(B)** and corresponding whole cell I_m recordings **(A and C)** from the same cells as in Figures 1, 2. Cell 1 I_m showed a quasilinear relationship, indicating low variability of membrane conductance **(A)**. In contrast, cell 2 I_m displayed rectification, consisting of larger I_m values at high positive voltages than at their negative counterparts **(C)**. This indicates the appearance of conductive membrane pathways (channels) at larger positive voltages. **(D, E)** Corresponding *I-V* plots for each cell, showing the values of initial I_m (first 30 ms; red triangles) and steady-state I_m (last 200 ms; blue dots). For both cells, the times where initial and steady-state I_m were measured are indicated in **(A)** by a red and a blue line, respectively. Notice that the non-linear increase of I_m in cell two starts around +50 mV, as expected from Cx43 hemichannels. The presence of Cs^+ in both internal and external solutions makes the conductivity of K^+ channels highly improbable.

3.3 Characterization of channel conductance using combined whole-cell and cell-attached recordings

Recognizing and measuring channel events within the large GSK-induced I_m is technically strenuous and most likely futile. To better document the conductance of the triggered channels, the response to the TRPV4 activation by GSK was further examined by combining whole-cell (WC) and cell-attached (CA) recordings, an approach effectively used before (Ek-Vitorin et al., 2023). In this technique, we use a patch pipette to achieve WC configuration in a selected cell, then approach a second patch pipette to achieve CA configuration in the same cell. Figure 5A illustrate the procedure (achievement of a high resistance seal in CA mode), after which we are able to record the total I_m while simultaneously capturing single channel events in a small patch on the same cell (inset in Figure 5A). Channel events were present in the WC recording before the formation of the CA patch (Figure 5B), and persist on further

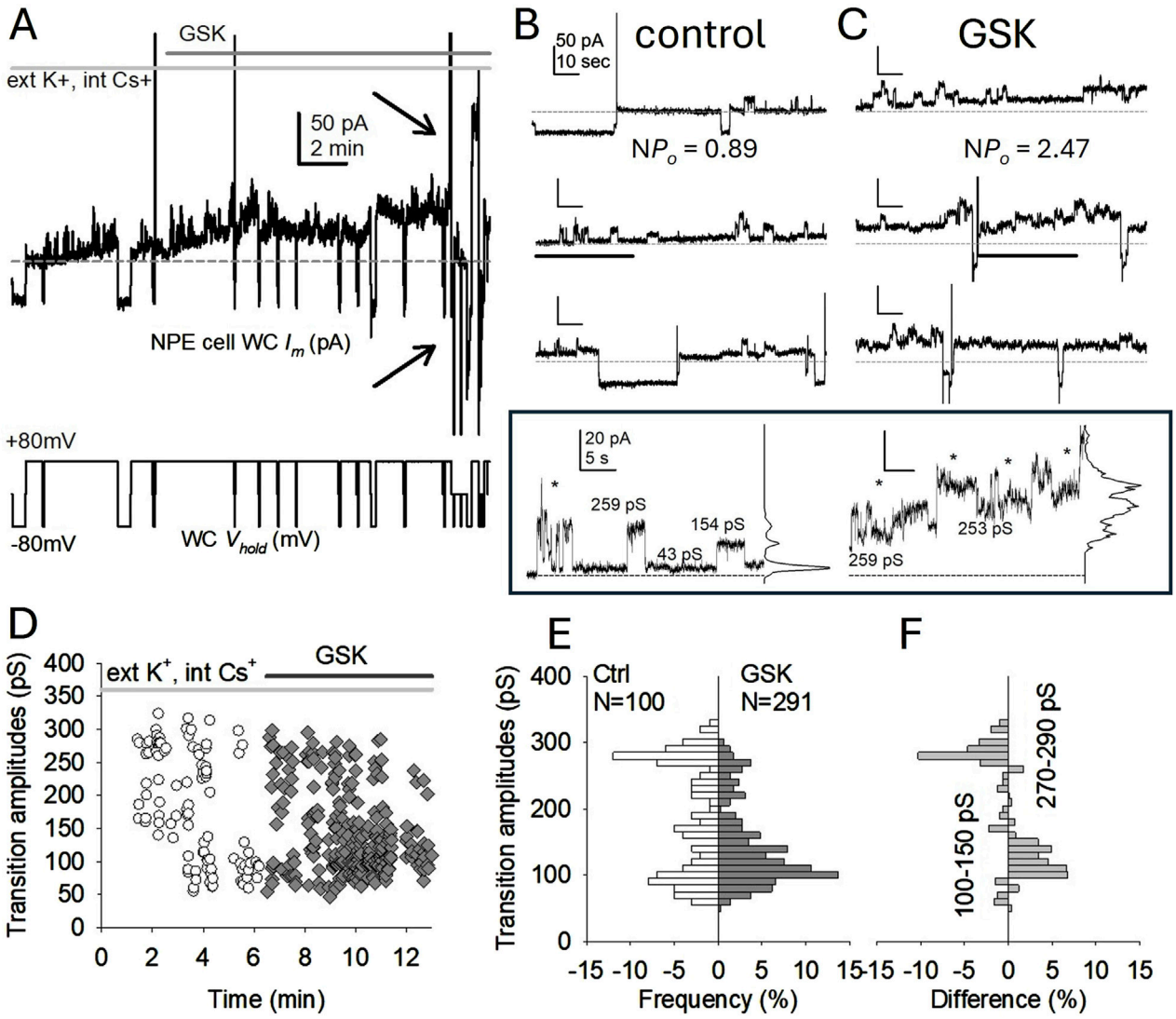

FIGURE 4
Cx43 hemichannel-like activity increases after TRPV4 activation. **(A)** Initial minutes of WC I_m recording from an experiment where TRPV4 agonist GSK1016790A (GSK, 10 nM) was added while applying long +80 mV, with short excursions to −80 mV to monitor overall I_m (bottom trace). The lowest initial I_m value is the baseline (dashed line) for this fragment. The whole cell I_m (top trace) seems to increase right after GSK application (time indicated by the top dark gray line). Notice that channel events [expanded in panels **(B, C)** for clarity] become less defined as overall I_m gradually increases, and soon larger I_m increases appear (arrows). Recording was performed in the presence of external K^+ and internal Cs^+ (top light gray line). **(B, C)** Contiguous 2-min length close-ups of whole cell I_m in **(A)**, from 6 min previous **(B)** and 6 min following **(C)** GSK application. NP_o indicates the open probability (P_o) for an apparent number of channels/levels (N, 5 before and 6 after GSK). As overall I_m further increased, P_o analysis became impracticable. In all traces, the dashed gray lines marks the initial baseline and show the modest I_m increase after GSK. Except where otherwise indicated, I_m calibration in the top left trace in B applies to the others. The bottom (framed) two traces are enlargements from sections (indicated with black lines) in traces of control and GSK conditions, respectively, to further illustrate the changes in channel behavior; differences are highlighted by the corresponding all-points histograms. Asterisks mark the presence of some transitions smaller than expected for full open Cx43 hemichannel transitions, which are more abundant after GSK. Full open transitions are still visible, but become less clear, after GSK treatment. I_m calibration on the left trace applies to the contiguous. **(D)** Manually measured event transition (open and close) amplitudes from the traces illustrated in **(B)** and **(C)**, before (white circles) and after GSK (dark gray diamonds). **(E)** Amplitude histograms for the transitions illustrated in **(D)**, before (white, left) and after (dark gray, right) GSK treatment. The histogram on the left side of **(E)** do not denote negative frequencies; this plotting device visually evince differences between channel populations using a left-to-right **(A)** symmetry). N is the number of measured transitions. **(F)** Difference plot (GSK - Control) from **(E)** shows decrease of full open transitions and increase of substates (or transitions to a residual state) after TRPV4 activation. Also notice that during equivalent periods (6 min) more transitions are present after GSK than before.

recording after CA patch formation, as shown next (Figure 6). From the full channel activity in the whole cell, only a few channels are expected to appear simultaneously on the CA patch. Figure 6 shows representative recordings from three different cells where GSK was present inside the CA patch pipette. Once the CA/WC configuration was attained, most of the events seen in the WC recording are not mirrored in the CA patch because they are occurring on other parts of the cell membrane. In contrast, channel events in the CA patch are necessarily mirrored in the WC recording because channels in the patch contribute to the whole cell channel activity. By including GSK in the patch electrode, the TRPV4 agonist was present only in the outer (extracellular) side of the patch and the observed channels

10.3389/frbis.2025.1543172

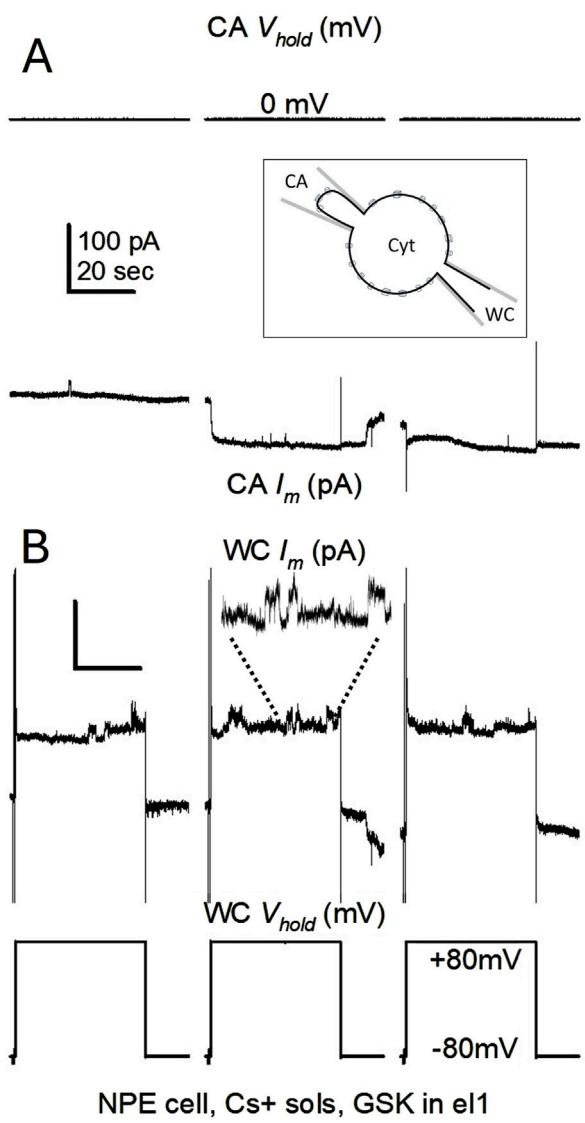

FIGURE 5
CA/WC configuration. **(A, B)** Illustration of a cell-attached (CA) seal formation in a cell already in whole-cell (WC) configuration. In **(A)**, V_m and I_m during the formation of a high resistance seal on a single cell. In **(B)**, I_m and V_m of the same whole cell. Pulses were applied from −80 to +80 mV to the whole cell side, and GSK1016790A (10 nM) was present inside the CA electrode (el1). The three pulses are contiguous in time and show the speed of seal formation, making GSK readily available to the membrane patch. The inset in **(A)** is a schematic of the settled CA/WC configuration in a single cell, whereby a fraction of the WC channel activity can be recorded through the CA pipette. Cyt denotes the cytoplasmic space. Hemichannel-like transitions were readily seen on whole cell I_m during CA attainment. An amplified 20-s stretch of I_m during the second pulse illustrate the appearing events. I_m calibration in **(A)** applies to **(B)**.

were probably GSK-induced. Notice that many events resembling connexin hemichannels, however blurred, are present in the WC I_m recording, and their frequency appear to increase, possibly because the GSK permeates through the membrane patch. In contrast, few channels occur in a CA patch, since that membrane fragment is a small portion of a much larger cell, and must contain fewer channels than the whole cell membrane. However, channels recorded in the CA patch are more defined than in the whole cell I_m and provide an accurate measurement of their amplitude, which is the goal of the procedure. The size of some channels in the CA patch is similar to the smaller-than-full-open transitions (≥100 pS) shown in Figures 4D, E. Smaller conductance transitions (25, 37, 62, 75 pS) can also be seen in the CA recordings, which are impossible to detect within the whole cell I_m and may represent TRPV4 channels (Earley, 2010). At this stage, the data agree with the expectation that activation of both TRPV4 channels and connexin hemichannel-like events are induced by GSK treatment.

3.4 Comparison of hemichannel and gap junction conductance

Cx43 and Cx50 are present in the ciliary epithelium (Shahidullah and Delamere, 2014; Li et al., 2018) and conductances of their respective gap junction channels are known (Ek-Vitorin and Burt, 2013; Harris, 2001). To reiterate, the conductance of an unpaired hemichannel is twice the conductance (half the resistance) of a gap junction channel. To determine whether Cx43 or Cx50 form functional hemichannels that respond to TRPV4 activation in NPE cells, we compared the amplitude of gap junction channels and presumptive hemichannels. Using dual voltage clamp (Ek-Vitorin and Burt, 2005) in cell pairs, gap junction channel conductance (γ_j) was measured between coupled NPE cells at a transjunctional voltage (V_j) of ±40 mV. Under these conditions, gap junction channel transition amplitudes corresponded to those expected from Cx43 (Figures 7A, C) and few transitions <100 pS were observed. At V_j = ±80 mV the relative frequency of fully open transitions decreased, and intermediate and residual transitions appeared (Figures 7B, C). These conductance shifts upon large V_j gradient is a well-known characteristic of Cx43 gap junction channels related to their voltage gating. Briefly, a fast-gating mechanism activated by large V_j gradients enhances transitions between the fully open and a residually open state, and between this residual and the fully closed state (Ek-Vitorin and Burt, 2013; Bukauskas et al., 2002; Ek-Vitorin et al., 2018; Gonzalez et al., 2007; Moreno et al., 2002). A corollary of these observations is that hemichannel transitions corresponding to those intermediate and smaller open states might be expected. This was the case. A comparison of the doubled conductances of gap junction channels ($2{\cdot}\gamma_j$) at V_j = ±80 mV (from Figure 7C) with the hemichannel conductances (Figure 7D, right) at V_m = +80 mV, reveals a similar range of amplitudes for both populations. These findings support the notion that NPE hemichannels are mainly composed of Cx43 and they display intermediate states. Together with the previous observations (Figures 4, 7), these results suggest that GSK increases both the frequency of hemichannel opening to an intermediate conductive state and/or the visits to a residual state.

3.5 TRPV4 activation increased I_m and decreased resting potential

We showed earlier that TRPV4 activation strongly and swiftly depolarizes lens epithelial cells, while increasing overall I_m (Ek-

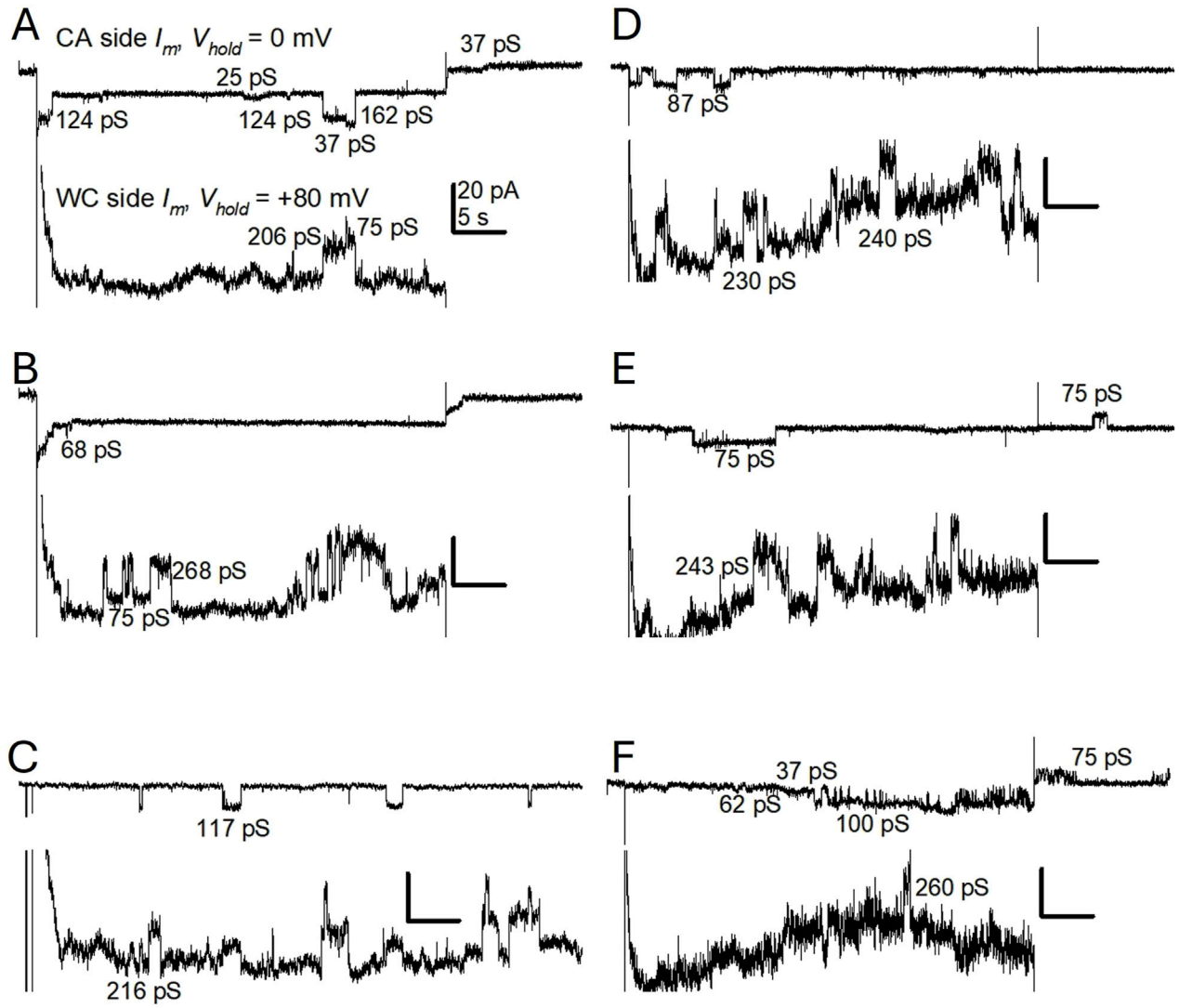

FIGURE 6
Channel activity on porcine NPE cell membrane contains events smaller than fully open Cx43-like hemichannels. **(A–F)** Except where indicated, shown are I_m recordings resulting from voltage pulsing as in Figure 5 (WC side: initial holding potential (V_{hold}) = −80 mV, pulsing 50 s to +80 mV every 60 s; CA side: kept at 0 mV). On each panel, the top trace is from the CA side, and the bottom trace is the WC I_m, showing channel activity in the whole cell membrane. V_{hold} values indicated in (A) apply to all panels, and GSK1016790A (GSK, 10 nm) is present on the CA side. Events are readily detectable and measurable on the CA side, and sometimes mirrored on the WC side; however, the events are blurred in the WC side by the more abundant channel activity of the whole membrane, as I_m increases. Calculated γ for some measurable events on the CA side is provided. A-B, C, and D-F are from three different cells. The trace in C comes from a longer +80 mV pulse. Notice that channels in **(E, F)** in the membrane patch (CA side) are longer but of smaller amplitude, and that some events are seen upon returning to −80 mV.

Vitorin et al., 2023). We observed that TRPV4 activation does not readily increase I_m in NPE cells pulsed to negative polarities. To examine the effect of TRPV4 activation more closely on negatively polarized NPE cells, we omitted the K^+ channel blocker Cs^+ from the electrode filling solution and from the bathing solution, and applied the TRPV4 agonist GSK while continuously holding the cell at V_m = −50 mV in WC configuration. This resulted in a gradual I_m increase that became larger (however, no more than two-fold) after >10 min of exposure to GSK (Figure 8A). This response is quantitatively different (smaller) than that in cells clamped at +80 mV. In a parallel series of experiments, the resting membrane potential (RMP) of grouped NPE cells was measured and found to be relatively small (−18.8 ± 0.9 mV; n = 20). When NPE cell groups (n = 9) were exposed to GSK, a biphasic depolarization ensued (Figure 8B). In control conditions, the baseline RMP was near −20 mV, and was halved upon GSK application.

While the observed I_m changes in GSK-treated cells held at −50 mV were modest, small channel-like transitions could be recognized, and their frequency appear to increase upon exposure to GSK (Figures 8C, D). The transitions, with conductances of 50–60 and 100–110 pS, resemble those observed in the CA/WC patch clamp configuration. These observations suggest that, in negatively polarized cells, GSK treatment leads to the opening of channels with amplitudes compatible to TRPV4, and other channels of larger amplitude that may represent connexin hemichannels of

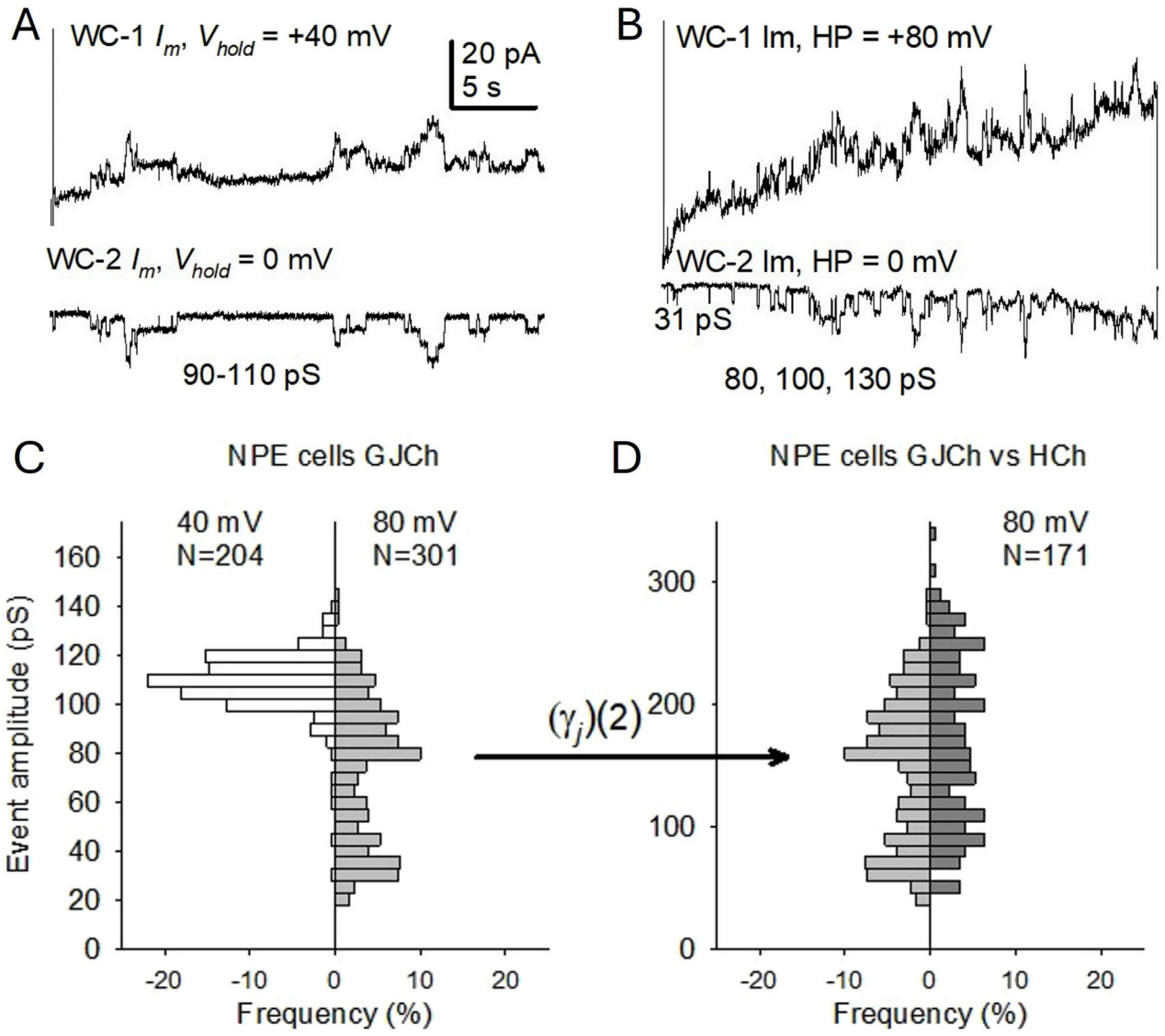

FIGURE 7
Hemichannel-like event amplitudes correspond to those of gap junction channels in porcine NPE cell pairs under control conditions. **(A, B)** Gap junction channel transitions in paired NPE cells. On each panel, the upper trace is the WC I_m on the pulsed cell, and the lower trace is the current changes recorded on the counterpart (non-pulsed) cell, representing the flow of ions through the gap junction channels. Transitions elicited by transjunctional voltages (V_j) of ±40 mV **(A)** and ±80 mV **(B)**, were measured on the non-pulsed cell. Conductance values of some measurable transitions are provided. I_m calibration in **(A)** applies to **(B)**. **(C)** Comparison of manually measured gap junction channel transition amplitudes (γ_j) at V_j values of ±40 mV (white, left) and ±80 mV (light gray, right). **(D)** Comparison of the expected transition amplitude range of hemichannels (gray, left, doubling of γ_j values at V_j = ±80 mV from **(C)**) and measured hemichannels transitions in NPE cells (dark gray, right) at V_m = +80 mV. N is the number of current (conductance) transitions. As in Figure 4, histograms on the left side of **(C, D)** do not denote negative frequencies, but are plotted to emphasize differences/similarities.

intermediate conductance. The combination of TRPV4 channels and hemichannels opening can explain the depolarization of the resting membrane potential in NPE cells.

4 Discussion

Previous studies made the case for functional hemichannels in the NPE based largely on indirect evidence such as propidium iodide uptake and the presence of unpaired connexin proteins on the basolateral surface that faces aqueous humor (Shahidullah and Delamere, 2014). The single cell patch clamp approach used here represents a more direct way to distinguish hemichannels by their unique electrical conductance. The goal of the present study was to detect and characterize connexin hemichannels in NPE cells. We also sought to determine whether activation of TRPV4 channels increases hemichannel opening, as previously proposed (Shahidullah and Delamere, 2023).

4.1 Evidence for hemichannels in the NPE

It was shown earlier that native and cultured porcine NPE expresses both Cx43 and Cx50. Cx43 was abundant at the

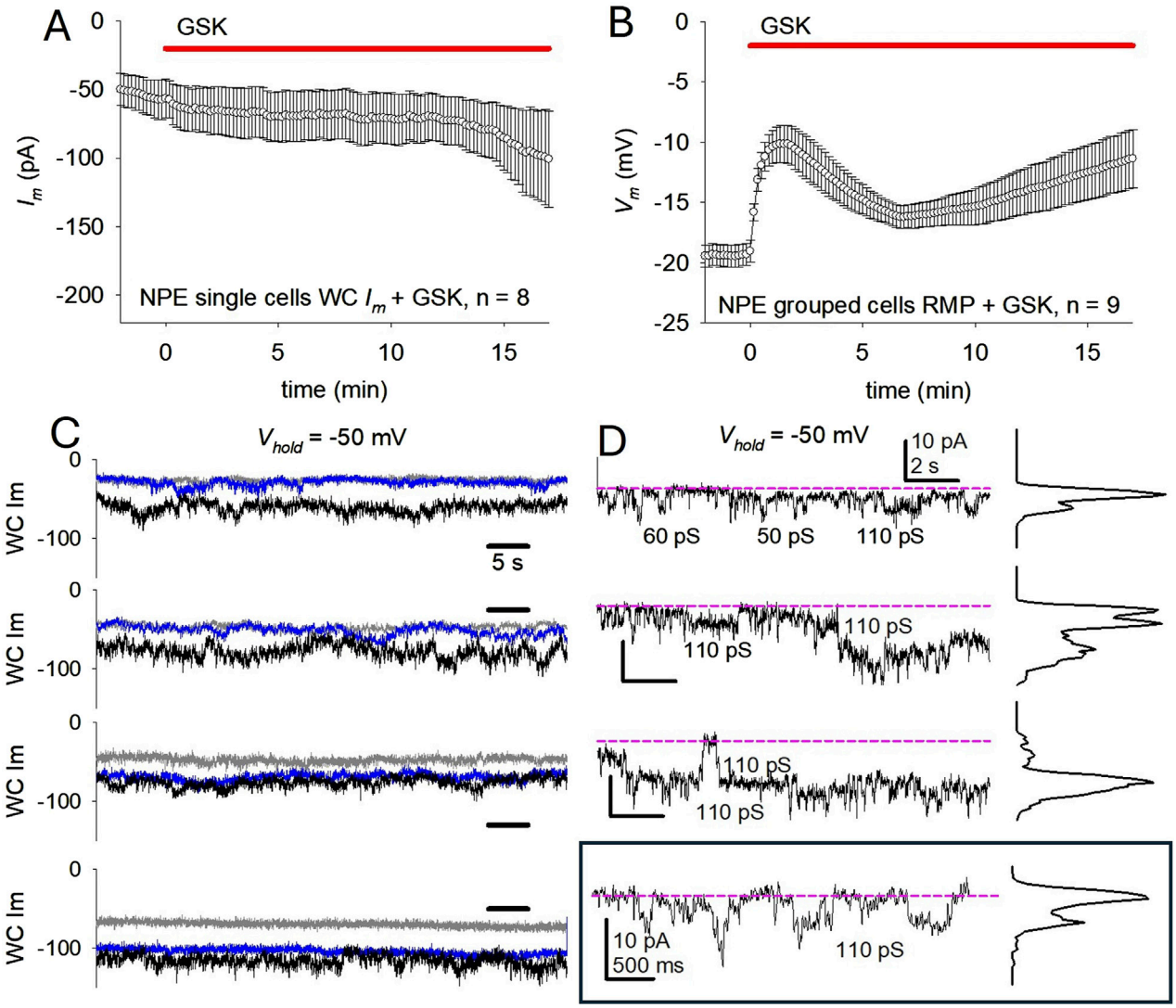

FIGURE 8
TRPV4 activation in porcine NPE cells increases membrane conductance and decreases membrane polarization. **(A)** Effect of TRPV4 activation on total I_m of single NPE cells at holding potential (V_{hold}) = −50 mV. An average I_m increase from ~-56 pA to ~ -85 pA was documented (n = 8) in the next 15 min. **(B)** Effect of TRPV4 activation on the resting membrane potentials (RMP) of grouped NPE cells. Average RMP was −19.0 ± 0.9 mV before GSK, and was depolarized to −10.2 ± 1.5 mV (n = 9) within 2 min of GSK application. Notice a partial recovery before a second prolonged depolarization phase. In **(A, B)**, the top red line indicate GSK (10 nM) application. **(C)** Samples of single NPE WC I_m before (gray), after 2 min (blue) and after 15 min (black) of GSK exposure illustrate the modest I_m increase. Time calibration in top trace applies to all traces. **(D)** Shorter samples of WC I_m from the third panel on **(C)**, before (top trace) and after (three next traces) exposure to GSK. The bottom (framed) trace was magnified to better display channel transitions. Except where otherwise indicated, calibration in top trace applies to all traces. The pink dashed lines serve as baselines for each segment, which from the top to the bottom trace are −25, −55, −60, and −70 pA respectively, illustrating the modest I_m increase. Notice the continual presence of recognizable, increasingly frequent, channel events. In these experiments, Cs^+ was excluded, and K^+-containing external and internal solutions were used.

junction between the NPE and PE layers, where gap junctions couple both cell types, while Cx50 was evident at the aqueous humor-facing, basolateral side of NPE (Shahidullah and Delamere, 2014). In the present study, several observations suggest that Cx43 probably forms functional hemichannels in NPE. Cultured single NPE cells displayed hemichannel-like activity evident as the opening of large conductance channels at +80 mV. Channel-like transitions observed in the range 180–240 pS are consistent with fully open Cx43 hemichannels (Contreras et al., 2003a; Ek-Vitorin et al., 2018). This hemichannel-like activity was variable and seldom occurred at negative holding potentials of −80 mV. Some cells showed little spontaneous activity unless the duration of the +80 mV pulse extended. It is generally known that Cx43 hemichannels remain (or become) closed at negative voltages, and that they open at values > +60 mV (Contreras et al., 2003a).

In coupled NPE cells, gap junction channels were observed with a main conductance ~120 pS that is consistent with Cx43 (Harris, 2001; Ek Vitorín et al., 2016); hemichannels formed by this connexin would have a maximal conductance of ~240 pS. In contrast, Cx50 gap junction channels would typically be characterized by a higher, ~200 pS conductance (Harris, 2001; Srinivas et al., 1999), and their expected hemichannel conductance would be ~400 pS. Thus, the conductance range of presumptive hemichannel transitions in

single NPE cells aligns well with Cx43. However, we also showed some hemichannel-like transitions with conductances larger than expected for Cx43 hemichannels (>250 pS), raising the possibility that a fraction of NPE hemichannels exist as heteromers of Cx43 and Cx50. This notion is supported by previous reports that heteromeric gap junction channels form when Cx43 and Cx40 are co-expressed (Cottrell et al., 2002). To be clear, the majority of the observed hemichannel-like transitions were within the conductance range expected for Cx43 even though the recordings also included conductances that correspond to substates or transitions to residual states, and some were slightly above the conductance expected for Cx43.

4.2 TRPV4 and hemichannels

Exposing the NPE cells to the TRPV4 agonist GSK1016970A increased the open probability of hemichannel-like events. The patch clamp findings align with previous indications that TRPV4 activation leads to hemichannel opening (Shahidullah and Delamere, 2014). For example, TRPV4 activation leads to a pattern of ATP release sensitive to the nonselective connexin blocker glycyrrhetinic acid, the connexin mimetic peptide GAP27, and a TRPV4 antagonist (Shahidullah and Delamere, 2023; Shahidullah et al., 2012a). Given the effect of voltage on hemichannels described above, we expected the effects of GSK on hemichannel-like events would be more apparent in cells polarized to positive voltage and this was the case.

It was noteworthy that in addition to increasing the open probability (P_o) of hemichannel-like events, cells responded to an extended period of GSK exposure by developing a large and sometimes catastrophic increase in membrane conductance. This likely reflects the persistent activation of TRPV4 channels by the agonist, and the resultant continuous increase of hemichannel P_o. It is interesting that such large membrane conductance becomes evident at high positive voltages, but not at negative voltages. To understand these observations, it is helpful to keep in mind that the biophysical conditions employed in our studies were designed to reveal changes in hemichannel activity and are far from physiological. Thus, cells were either held at positive voltage values where they are unlikely to dwell in normal circumstances, or they were held at negative potentials where hemichannels would remain closed. Interestingly, when cells were not voltage-clamped, TRPV4 activation shifted the resting potential to more depolarized values, effectively decreasing an influential factor that keeps hemichannels closed. Depolarization increases Cx43 hemichannel open probability (Contreras et al., 2003a) and it is worth remembering that in previous studies, the hemichannel-mediated ATP release and propidium iodide uptake observed after GSK-induced TRPV4 activation occurred while the cell membrane resting potential was free to depolarize.

Identifying the mechanistic link between TRPV4 channel activation and Cx43 hemichannels opening is beyond the scope of the current studies. However, it is likely that such mechanism involves an increase of intracellular Ca^{2+} (De Vuyst et al., 2009; Bayraktar et al., 2024) caused by entry of extracellular Ca^{2+} when TRPV4 channels are activated. Indeed, TRPV4 permits significant Ca^{2+} entry (Sánchez-Hernández et al., 2024). It is clear, however, that hemichannel opening is not associated with Ca^{2+} entry via other channels such as TRPM3, TRPV1 and Piezo1 (Shahidullah and Delamere, 2023; Delamere and Shahidullah, 2021). One possible explanation is that TRPV4 activation causes localized Ca^{2+} entry in close proximity to hemichannels. (While this manuscript was in review, an elegant new study appeared in which the authors demonstrate close proximity of Cx43 and TRPV4 in primary cultured endothelial cells from resistance arteries. In that tissue, TRPV4 activation enhances eNOS activity and Cx43 hemichannels open as a result of S-nitrosylation (Burboa et al., 2025).

The present study showed depolarization of NPE cells in response to TRPV4 activation by GSK, and depolarization *per se* increases hemichannel open probability (Contreras et al., 2003a). This GSK-induced depolarization was, in absolute values, smaller than that observed in lens cells (Ek-Vitorin et al., 2023). However, GSK reduced the magnitude of the resting potential by 50%, depolarizing NPE cells closer to 0 mV. Voltage effects have been studied in gap junctions and it is well known that the maximum number of open gap junction channels appears at small V_j values (Gonzalez et al., 2007), when both connexons are conductive. At larger V_j values gap junction channels close, and different connexins may respond to polarity in diverse ways. Cx43 connexons close at negative voltages but open at positive polarization (Elenes et al., 2001). In contrast, Cx50 hemichannels may not open at large positive membrane voltages (Ebihara et al., 1999; Hopperstad et al., 2000; Beahm and Hall, 2002), but may open at large negative values. Of particular interest in this regard is a study (Beahm and Hall, 2002) in frog oocytes that showed small Cx50 hemichannel currents in 2 mM Ca^{2+}, and an increase of these currents when Ca^{2+} was lowered to 0.2 mM. However, the normalized conductance of the presumed Cx50 hemichannel currents showed a maximal steady-state between −40 and +20 mV. These hemichannels appeared to gate (close) at larger positive or negative voltages but did so much faster at positive voltages. Thus, the authors suggested that (connexons in) Cx50 gap junctions "gate with positive relative polarity". In our conditions, Cx43 but not Cx50 hemichannels may open at membrane potentials that are largely positive, while at values near 0 mV, as occurs after GSK-induced TRPV4 activation, both Cx43 and Cx50 hemichannels could be operational. Under physiological settings, regional depolarizations in the NPE layer are probably limited in time and space, because the stimulus would not be persistent and because electrotonic interaction through gap junctions with neighboring, non-depolarized cells would bring the resting potential back to normal values.

4.3 Connexin 43

Under the conditions of our study, TRPV4 activation caused an increase in the open probability of hemichannels that have a conductance typical of Cx43. Different connexins have characteristic conductances and differ in other functional attributes such as permselectivity. For example, gap junctions formed by Cx43 display no charge selectivity (Ek Vitorín et al., 2016; Heyman et al., 2009) and are more permeable than those of

Cx50 to molecules larger than atomic ions (Dong et al., 2006). In addition, Cx50 gap junctions may be impermeable to negatively charged molecules (Valiunas and White, 2020). Assuming that the attributes of connexons in gap junction channels and hemichannels are similar, Cx43 hemichannels are reasonably expected to allow the transmembrane movement of both positively charged molecules like propidium iodide and negatively charged molecules such as ATP and IP3. In contrast Cx50 hemichannels would be positive-selective but negative-restrictive.

The results also suggest the possibility that GSK induces the appearance of Cx43 hemichannels with intermediate or low conductance. Previous studies on permeability and electrical conductance of single Cx43 gap junction channels have suggested there may be mechanisms that differentially regulate the single channel permeability for larger molecules and for small inorganic ions (Eckert, 2006). It was also shown that increasing the frequency of gap junction channel transitions of largest conductance reduces the permeability of gap junctions to small molecules of ~280 Da (Ek-Vitorin et al., 2006). In other words, intermediate electrical conductances, like those shown here, may be associated with higher channel permeability. An alternative explanation for the discrepancy between electrical conductance and permeability was proposed in a recent study that examined the permeability of hemichannels formed by Cx26 and Cx30 by measuring permeation of fluorescent probes. The authors identified differences in the way molecules and atomic ions passed through the hemichannels. Molecules but not ions exhibited uptake kinetics compatible with a saturable transporter-like mechanism (Gaete et al., 2024). Interestingly, mutants of Cx26 that displayed reduced ionic currents were still able to mediate dye uptake, leading to the conclusion that connexin hemichannels may independently act as ion channels and molecule transporters (Gaete et al., 2024).

While the present patch clamp findings on cultured single NPE cells point to hemichannels formed by Cx43, earlier studies in the NPE of intact porcine eyes pointed to Cx50 as the more abundant unpaired connexin (Wolosin et al., 1997). Newer studies indicate Cx43 is the most abundant (up to 200-fold) of five different connexins present in the ciliary body, although Cx43 was primarily localized in the PE-NPE interface and the basolateral membranes of PE cells (Li et al., 2018). Importantly, while immunostaining affords a good general impression of protein distribution within tissues, it may fail to detect low expression levels. In contrast, patch clamp can demonstrate the function of even a single, otherwise undetectable channel. It should also be kept in mind that there are many differences between an intact epithelial tissue and cells in primary culture. Connexin localization must be quite different in cultured cells that lack well-defined polarization into basolateral and apical domains. As a consequence, connexin responses may be quite different in single cells. Moreover, it might be overly simplistic to think hemichannels are formed exclusively by either Cx43 or Cx50. In short, the role of Cx50 hemichannels in the exchange of intracellular and extracellular components, especially after TRPV4 activation, cannot be ruled out. Future studies are needed to consider the above stated possibility of Cx43 and Cx50 heteromerization which could yield gap junctions or hemichannels of mixed functional features.

4.4 Functional relevance of hemichannels at the basolateral surface of NPE

Hemichannel opening at the basolateral surface of NPE cells would introduce a pathway for the exchange of molecules between the interior of the epithelium and the aqueous humor. This exchange, if massive or prolonged, would likely be deleterious to ion homeostasis in the NPE cells themselves. However, a spatially controlled and time-limited increase of hemichannel open probability would allow fine-tuning of basolateral membrane permeability that could be valuable for a fluid transporting cell. Basolateral hemichannels formed by Cx43, would be a conduit for atomic and molecular ions as large as 1.2 kDa (e.g., glucose, glutathione, ATP, AMP, amino acids) to pass from the NPE cell into aqueous humor.

Previous studies of hemichannels in the intact eye pointed out to a baseline level of hemichannel opening as evidenced by significant basal uptake of propidium iodide by NPE cells (Shahidullah and Delamere, 2014; Shahidullah and Delamere, 2023). Moreover, NPE cells display a measurable degree of ATP release under control conditions (Shahidullah and Delamere, 2023). This may reflect a low-level steady-state of hemichannels flickering open spontaneously, that is consistent with the hemichannel activity in control conditions shown here.

The 2 cell layers of ciliary (pigmented and non-pigmented) epithelium operate in coordination to form aqueous humor. PE and NPE are equipped with different transport mechanisms. Remarkably, PE but not NPE cells characteristically exhibit a regulatory volume increase when subjected to osmotic shrinkage (Edelman et al., 1994). In contrast, NPE but not PE cells exhibit a regulatory volume decrease when subjected to osmotic swelling (Edelman et al., 1994). On this basis, the PE appears specialized for solute entry while the NPE is specialized for solute exit (Edelman et al., 1995; Walker et al., 1999). The cells are coupled by gap junctions, and solute and water move through the bilayer at such a rate that an NPE cell transports the equivalent of 30% of its own volume every minute (Brubaker, 1991). It is reasonable to consider that the cells are at risk of swelling or shrinkage if there were a mismatch between entry and exit of water that flows through them. Activation of TRPV4 in response to cell swelling, and a consequent increase of the open probability of connexin hemichannels, may have a role in maintenance of cell volume homeostasis. Jo and coworkers (Jo et al., 2016) reported swelling-induced calcium responses in the NPE. The same study showed prevention of the swelling-induced calcium responses by TRPV4 inhibition in mouse NPE and absence of these responses in the TRPV4 knockout mice. Interestingly, it has been reported that GSK1016790A reduces intraocular pressure (IOP) in mice (Luo et al., 2014). In the same study, TRPV4 knockout mice were found to have elevated IOP. However, others have reported that IOP is normal in TRPV4 knockout mice (Ryskamp et al., 2016).

5 Conclusion

Primary cultured porcine non-pigmented epithelial cells show spontaneous hemichannel activity. Agonist activation of TRPV4 may increase hemichannel open probability and decrease hemichannel conductance. Certainly, further pharmacological agonist-antagonist studies are needed to better establish the connection between TRPV4 activation and Cx43 hemichannel activity. However, it can be stated that the hemichannel-like activity in this study shows electrical properties matching those of Cx43. The results are consistent with

reports that suggest TRPV4 channel activation, by mechanical stimuli associated with cell swelling, has a stimulatory effect on connexin hemichannel opening.

Data availability statement

The raw data supporting the conclusions of this article will be made available by the authors, without undue reservation.

Ethics statement

The animal study was approved by Institutional Animal Care and Use Committee (IACUC) of the Animal Welfare Program (AWP) at the University of Arizona. The study was conducted in accordance with the local legislation and institutional requirements.

Author contributions

JE-V: Conceptualization, Data curation, Formal Analysis, Investigation, Methodology, Visualization, Writing – original draft, Writing – review and editing. MS: Conceptualization, Validation, Writing – review and editing. ND: Conceptualization, Funding acquisition, Project administration, Resources, Supervision, Validation, Visualization, Writing – review and editing.

Funding

The author(s) declare that financial support was received for the research and/or publication of this article. This work was supported by Grants R01EY029171, R01EY09532.

Conflict of interest

The authors declare that the research was conducted in the absence of any commercial or financial relationships that could be construed as a potential conflict of interest.

Generative AI statement

The author(s) declare that no Generative AI was used in the creation of this manuscript.

Publisher's note

Supplementary material

The Supplementary Material for this article can be found online at: https://www.frontiersin.org/articles/10.3389/frbis.2025.1543172/full#supplementary-material

SUPPLEMENTAL FIGURE S1
Whole cell membrane currents (WC I_m) from single porcine nonpigmented ciliary Epithelial (NPE) cell, in the presence of external K^+ and internal Cs^+, during pulses at −80 and +80 mV. Notice the narrow capacitive currents both during the large pulses and the smaller (±10 mV) prepulses. In this example, a channel-like event (asterisk) is evident during the +80 mV pulse.

SUPPLEMENTAL FIGURE S2
Whole cell membrane current (WC I_m) recording fragment showing the typical behavior of connexin hemichannel-like transitions at +80 mV in control conditions. The recording is from a single porcine NPE cell, in the presence of external K^+ and internal Cs^+. The trace displays an initial slow opening (upwards, pink arrow) from a baseline (dashed line), followed by multiple, faster, openings and closures. Notice that the subsequent transitions occur from and to persistent levels different from the baseline, and which may represent channels continuously open to residual conductive states. In accord, openings and closures of smaller amplitude are also present: two conspicuous examples of these are marked by asterisks. Notice that the time the presumptive hemichannels remain open (dwell time) is variable. Analogous operation of connexin channels (both gap junction and connexons) has been widely reported in other cell types (see for instance (Ek-Vitorin et al., 2023; Contreras et al., 2003a; Ek-Vitorin et al., 2018) referenced in the main text).

References

Bayraktar, E., Lopez-Pigozzi, D., and Bortolozzi, M. (2024). Calcium regulation of connexin hemichannels. *Int. J. Mol. Sci.* 25, 6594. doi:10.3390/ijms25126594

Beahm, D. L., and Hall, J. E. (2002). Hemichannel and junctional properties of connexin 50. *Biophysical J.* 82, 2016–2031. doi:10.1016/s0006-3495(02)75550-1

Brubaker, R. F. (1991). Flow of aqueous humor in humans [The Friedenwald Lecture]. *Invest Ophthalmol. Vis. Sci.* 32, 3145–3166.

Bukauskas, F. F., Bukauskiene, A., and Verselis, V. K. (2002). Conductance and permeability of the residual state of connexin43 gap junction channels. *J. General Physiology* 119, 171–186. doi:10.1085/jgp.119.2.171

Burboa, P. C., Gaete, P. S., Shu, P., Araujo, P. A., Beuve, A. V., Durán, W. N., et al. (2025). Endothelial TRPV4-Cx43 signalling complex regulates vasomotor tone in resistance arteries. *J. Physiol.* doi:10.1113/JP285194

Contreras, J. E., Saez, J. C., Bukauskas, F. F., and Bennett, M. V. (2003a). Gating and regulation of connexin 43 (Cx43) hemichannels. *Proc. Natl. Acad. Sci. U. S. A.* 100, 11388–11393. doi:10.1073/pnas.1434298100

Contreras, J. E., Sáez, J. C., Bukauskas, F. F., and Bennett, M. V. (2003b). Functioning of cx43 hemichannels demonstrated by single channel properties. *Cell Commun. Adhes.* 10, 245–249. doi:10.1080/cac.10.4-6.245.249

Cottrell, G. T., Wu, Y., and Burt, J. M. (2002). Cx40 and Cx43 expression ratio influences heteromeric/heterotypic gap junction channel properties. *Am. J. Physiology-Cell Physiology* 282, C1469–C1482. doi:10.1152/ajpcell.00484.2001

Delamere, N. A., and Shahidullah, M. (2021). Ion transport regulation by TRPV4 and TRPV1 in lens and ciliary epithelium. *Front. Physiol.* 12, 834916. doi:10.3389/fphys.2021.834916

De Vuyst, E., Wang, N., Decrock, E., De Bock, M., Vinken, M., Van Moorhem, M., et al. (2009). Ca(2+) regulation of connexin 43 hemichannels in C6 glioma and glial cells. *Cell Calcium* 46, 176–187. doi:10.1016/j.ceca.2009.07.002

Dong, L., Liu, X., Li, H., Vertel, B. M., and Ebihara, L. (2006). Role of the N-terminus in permeability of chicken connexin45.6 gap junctional channels. *J. Physiology* 576, 787–799. doi:10.1113/jphysiol.2006.113837

Earley, S. (2010). Vanilloid and melastatin transient receptor potential channels in vascular smooth muscle. *Microcirculation* 17, 237–249. doi:10.1111/j.1549-8719.2010.00026.x

Ebihara, L., Xu, X., Oberti, C., Beyer, E. C., and Berthoud, V. M. (1999). Co-expression of lens fiber connexins modifies hemi-gap-junctional channel behavior. *Biophysical J.* 76, 198–206. doi:10.1016/s0006-3495(99)77189-4

Eckert, R. (2006). Gap-junctional single-channel permeability for fluorescent tracers in mammalian cell cultures. *Biophysical J.* 91, 565–579. doi:10.1529/biophysj.105.072306

Edelman, J. L., Loo, D. D., and Sachs, G. (1995). Characterization of potassium and chloride channels in the basolateral membrane of bovine nonpigmented ciliary epithelial cells. *Invest Ophthalmol. Vis. Sci.* 36, 2706–2716.

Edelman, J. L., Sachs, G., and Adorante, J. S. (1994). Ion transport asymmetry and functional coupling in bovine pigmented and nonpigmented ciliary epithelial cells. *Am. J. Physiology-Cell Physiology* 266, C1210–C1221. doi:10.1152/ajpcell.1994.266.5.c1210

Ek-Vitorin, J. F., and Burt, J. M. (2005). Quantification of gap junction selectivity. *Am. J. Physiology-Cell Physiology* 289, C1535–C1546. doi:10.1152/ajpcell.00182.2005

Ek-Vitorin, J. F., and Burt, J. M. (2013). Structural basis for the selective permeability of channels made of communicating junction proteins. *Biochimica Biophysica Acta (BBA) - Biomembr.* 1828, 51–68. doi:10.1016/j.bbamem.2012.02.003

Ek-Vitorin, J. F., King, T. J., Heyman, N. S., Lampe, P. D., and Burt, J. M. (2006). Selectivity of connexin 43 channels is regulated through protein kinase C-dependent phosphorylation. *Circulation Res.* 98, 1498–1505. doi:10.1161/01.res.0000227572.45891.2c

Ek-Vitorin, J. F., Pontifex, T. K., and Burt, J. M. (2018). Cx43 channel gating and permeation: multiple phosphorylation-dependent roles of the carboxyl terminus. *Int. J. Mol. Sci.* 19, 1659. doi:10.3390/ijms19061659

Ek-Vitorin, J. F., Shahidullah, M., Lopez Rosales, J. E., and Delamere, N. A. (2023). Patch clamp studies on TRPV4-dependent hemichannel activation in lens epithelium. *Front. Pharmacol.* 14, 1101498. doi:10.3389/fphar.2023.1101498

Ek Vitorín, J., Pontifex, T. K., and Burt, J. M. (2016). Determinants of Cx43 channel gating and permeation: the amino terminus. *Biophysical J.* 110, 127–140. doi:10.1016/j.bpj.2015.10.054

Elenes, S., Martinez, A. D., Delmar, M., Beyer, E. C., and Moreno, A. P. (2001). Heterotypic docking of Cx43 and Cx45 connexons blocks fast voltage gating of Cx43. *Biophysical J.* 81, 1406–1418. doi:10.1016/s0006-3495(01)75796-7

Gaete, P. S., Kumar, D., Fernandez, C. I., Valdez Capuccino, J. M., Bhatt, A., Jiang, W., et al. (2024). Large-pore connexin hemichannels function like molecule transporters independent of ion conduction. *Proc. Natl. Acad. Sci. U. S. A.* 121, e2403903121. doi:10.1073/pnas.2403903121

Ghosh, S., Hernando, N., Martín-Alonso, J. M., Martin-Vasallo, P., and Coca-Prados, M. (1991). Expression of multiple Na+,K(+)-ATPase genes reveals a gradient of isoforms along the nonpigmented ciliary epithelium: functional implications in aqueous humor secretion. *J. Cell Physiol.* 149, 184–194. doi:10.1002/jcp.1041490203

Gonzalez, D., Gomez-Hernandez, J. M., and Barrio, L. C. (2007). Molecular basis of voltage dependence of connexin channels: an integrative appraisal. *Prog. Biophysics Mol. Biol.* 94, 66–106. doi:10.1016/j.pbiomolbio.2007.03.007

Harris, A. L. (2001). Emerging issues of connexin channels: biophysics fills the gap. *Q. Rev. Biophys.* 34, 325–472. doi:10.1017/s0033583501003705

Heyman, N. S., Kurjiaka, D. T., Ek Vitorin, J. F., and Burt, J. M. (2009). Regulation of gap junctional charge selectivity in cells coexpressing connexin 40 and connexin 43. *Am. J. Physiology-Heart Circulatory Physiology* 297, H450–H459. doi:10.1152/ajpheart.00287.2009

Hopperstad, M. G., Srinivas, M., and Spray, D. C. (2000). Properties of gap junction channels formed by Cx46 alone and in combination with Cx50. *Biophysical J.* 79, 1954–1966. doi:10.1016/s0006-3495(00)76444-7

Jo, A. O., Lakk, M., Frye, A. M., Phuong, T. T., Redmon, S. N., Roberts, R., et al. (2016). Differential volume regulation and calcium signaling in two ciliary body cell types is subserved by TRPV4 channels. *Proc. Natl. Acad. Sci. U. S. A.* 113, 3885–3890. doi:10.1073/pnas.1515895113

Li, S. K., Shan, S. W., Li, H. L., Cheng, A. K., Pan, F., Yip, S. P., et al. (2018). Characterization and regulation of gap junctions in porcine ciliary epithelium. *Invest Ophthalmol. Vis. Sci.* 59, 3461–3468. doi:10.1167/iovs.18-24682

Luo, N., Conwell, M. D., Chen, X., Kettenhofen, C. I., Westlake, C. J., Cantor, L. B., et al. (2014). Primary cilia signaling mediates intraocular pressure sensation. *Proc. Natl. Acad. Sci. U. S. A.* 111, 12871–12876. doi:10.1073/pnas.1323292111

Moreno, A. P., Chanson, M., Anumonwo, J., Scerri, I., Gu, H., Taffet, S. M., et al. (2002). Role of the carboxyl terminal of connexin43 in transjunctional fast voltage gating. *Circulation Res.* 90, 450–457. doi:10.1161/hh0402.105667

Riley, M. V., and Kishida, K. (1986). ATPases of ciliary epithelium: cellular and subcellular distribution and probable role in secretion of aqueous humor. *Exp. Eye Res.* 42, 559–568. doi:10.1016/0014-4835(86)90046-1

Ryskamp, D. A., Frye, A. M., Phuong, T. T., Yarishkin, O., Jo, A. O., Xu, Y., et al. (2016). TRPV4 regulates calcium homeostasis, cytoskeletal remodeling, conventional outflow and intraocular pressure in the mammalian eye. *Sci. Rep.* 6, 30583. doi:10.1038/srep30583

Sánchez-Hernández, R., Benítez-Angeles, M., Hernández-Vega, A. M., and Rosenbaum, T. (2024). Recent advances on the structure and the function relationships of the TRPV4 ion channel. *Channels* 18, 2313323. doi:10.1080/19336950.2024.2313323

Shahidullah, M., and Delamere, N. A. (2014). Connexins form functional hemichannels in porcine ciliary epithelium. *Exp. Eye Res.* 118, 20–29. doi:10.1016/j.exer.2013.11.004

Shahidullah, M., and Delamere, N. A. (2023). Mechanical stretch activates TRPV4 and hemichannel responses in the nonpigmented ciliary epithelium. *Int. J. Mol. Sci.* 24, 1673. doi:10.3390/ijms24021673

Shahidullah, M., Mandal, A., Beimgraben, C., and Delamere, N. A. (2012b). Hyposmotic stress causes ATP release and stimulates Na,K-ATPase activity in porcine lens. *J. Cell. Physiology* 227, 1428–1437. doi:10.1002/jcp.22858

Shahidullah, M., Mandal, A., and Delamere, N. A. (2012a). TRPV4 in porcine lens epithelium regulates hemichannel-mediated ATP release and Na-K-ATPase activity. *Am. J. Physiology-Cell Physiology* 302, C1751–C1761. doi:10.1152/ajpcell.00010.2012

Shahidullah, M., Tamiya, S., and Delamere, N. A. (2007). Primary culture of porcine nonpigmented ciliary epithelium. *Curr. Eye Res.* 32, 511–522. doi:10.1080/02713680701434899

Srinivas, M., Costa, M., Gao, Y., Fort, A., Fishman, G. I., and Spray, D. C. (1999). Voltage dependence of macroscopic and unitary currents of gap junction channels formed by mouse connexin50 expressed in rat neuroblastoma cells. *J. Physiology* 517 (Pt 3), 673–689. doi:10.1111/j.1469-7793.1999.0673s.x

Valiunas, V., and White, T. W. (2020). Connexin43 and connexin50 channels exhibit different permeability to the second messenger inositol triphosphate. *Sci. Rep.* 10, 8744. doi:10.1038/s41598-020-65761-z

Walker, V. E., Stelling, J. W., Miley, H. E., and Jacob, T. J. (1999). Effect of coupling on volume-regulatory response of ciliary epithelial cells suggests mechanism for secretion. *Am. J. Physiology-Cell Physiology* 276, C1432–C1438. doi:10.1152/ajpcell.1999.276.6.c1432

Wolosin, J. M., Schütte, M., and Chen, S. (1997). Connexin distribution in the rabbit and rat ciliary body. A case for heterotypic epithelial gap junctions. *Invest Ophthalmol. Vis. Sci.* 38, 341–348.